2-15-2014

Dice: Challenges of Spinning Cubesats

Tim Neilsen

Cameron Weston

Chad Fish

Bryan Bingham

Recommended Citation

Utah State University
MERRILL-CAZIER LIBRARY

AAS 14-068

DICE: CHALLENGES OF SPINNING CUBESATS

Tim Neilsen,[*] Cameron Weston,[†] Chad Fish,[‡] and Bryan Bingham[§]

Funded by the NSF CubeSat and NASA ELaNa programs, the DICE mission consists of two 1.5U CubeSats which were launched into an eccentric low Earth orbit on October 28th, 2011. Each identical spacecraft carries a suite of ionospheric space weather payloads. The use of two identical CubeSats, at slightly different orbiting velocities in nearly identical orbits, permits the deconvolution of spatial and temporal ambiguities in the observations of the ionosphere from a moving platform. Deployable wire booms require each CubeSat to be spin stabilized. Attitude determination and control are accomplished using magnetometers, a sun sensor, and torque coils. Position and time are provided by GPS.

DICE has greatly advanced nano-satellite based mission capabilities, demonstrating constellation science and opening up a number of groundbreaking technologies to the CubeSat community. DICE has made many co-incident observations of ionospheric structure and is the first CubeSat mission to observe field-aligned currents in the ionosphere. In this paper we will review the on-orbit performance of the DICE ADCS design as well as communications/GPS antenna issues associated with a spinning CubeSat.

INTRODUCTION

Sponsored by the National Science Foundation (NSF) CubeSat Space Weather and NASA ELaNa programs, the Dynamic Ionosphere CubeSat Experiment (DICE) mission[1] consists of a pair of identical 1.5U CubeSats launched into a 350 x 800 km low Earth orbit (LEO) on October 28th, 2011. Each spacecraft houses a suite of three science instruments, which measure ionospheric in-situ plasma densities, electric fields, and magnetic fields. The DICE PI is Geoff Crowley from ASTRA LLC. Utah State University/Space Dynamics Laboratory (USU/SDL) implemented the mission and provided mission operations.

The DICE mission consists of two 1.5U CubeSats—designated Farkle and Yahtzee. Each spacecraft instrument comprises two Electric Field Probe (EFP) pairs on long, flexible wire booms which measure in-situ electric fields, two Langmuir Probes (LP) on extendable scissor booms to measure

[*] Lead Engineer, DICE Program, Space Dynamics Lab / Utah State University, 1695 N Research Park Way, North Logan, UT 84341
[†] Electrical Engineer, DICE Program, Space Dynamics Lab / Utah State University, 1695 N Research Park Way, North Logan, UT 84341
[‡] Program Manager, DICE Program, Space Dynamics Lab / Utah State University, 1695 N Research Park Way, North Logan, UT 84341
[§] ADCS Lead, DICE Program, Space Dynamics Lab / Utah State University, 1695 N Research Park Way, North Logan, UT 84341

ionospheric in-situ plasma densities and temperature, and a science-grade magnetometer to measure in-situ magnetic fields.

Both spacecraft were ejected from the same P-Pod deployer with slightly different ejection velocities (due to small separation springs in the foot of each CubeSat and decreased plunger spring force for the second spacecraft—Yahtzee). The DICE spacecraft's initial orbital parameters are nearly identical with slightly different orbital velocities. This orbital configuration allows DICE to deconvolve the temporal-spatial ambiguity of ionospheric observations by allowing data analysis of measurements from one point in space and time to be compared to a subsequent measurement at a nearly identical location some minutes later.

One objective of the DICE mission is to serves as a pathfinder for low-cost, multi-point CubeSat constellation observations of the ionosphere. We expect in coming years that follow-on missions where dozens or perhaps hundreds of CubeSats with similar instrumentation will create a comprehensive network of measurements allowing truly global coverage of in-situ ionospheric measurements. This global network of measurements will allow us to understand the complex interaction between the Earth's upper atmosphere and highly dynamic solar activity.

Figure 1. Concept Drawing of DICE

SPACECRAFT DESCRIPTION

Key to the spacecraft's ability to measure in-situ electric fields is a pair of double probe electric fields sensors deployed on flexible wire booms. The four electric field probe booms each extend approximately 5 m from the spacecraft with electrically conductive spheres terminating each boom tip. The 5 m wire booms are deployed slowly from a modular spool designed for DICE, but with the intent of being reconfigurable for different wire diameters and lengths on future missions. The deployment and maintenance of relative spacing of these wire booms are the driving reasons for the requirement for a spinning spacecraft. Once a stable spacecraft spin of approximately 2 Hz is achieved, the spool slowly deploys over the course of days giving the spacecraft time to correct perturbations and maintain the proper spin rate (which degrades as the probe masses extend from the center of mass). Once fully deployed, the spin rate of approximately 0.1 Hz is maintained.

Proper on-orbit deployment of the electric field wire booms requires balance between centrifugal forces and mechanical friction of the spool and boom wire. As the sphere masses are pulled away from the spin axis, the spool brake motor takes steps allowing all four boom wires to extend a few millimeters per step. Small damping washers slowly damp out boom oscillations before another deployment step can be taken.
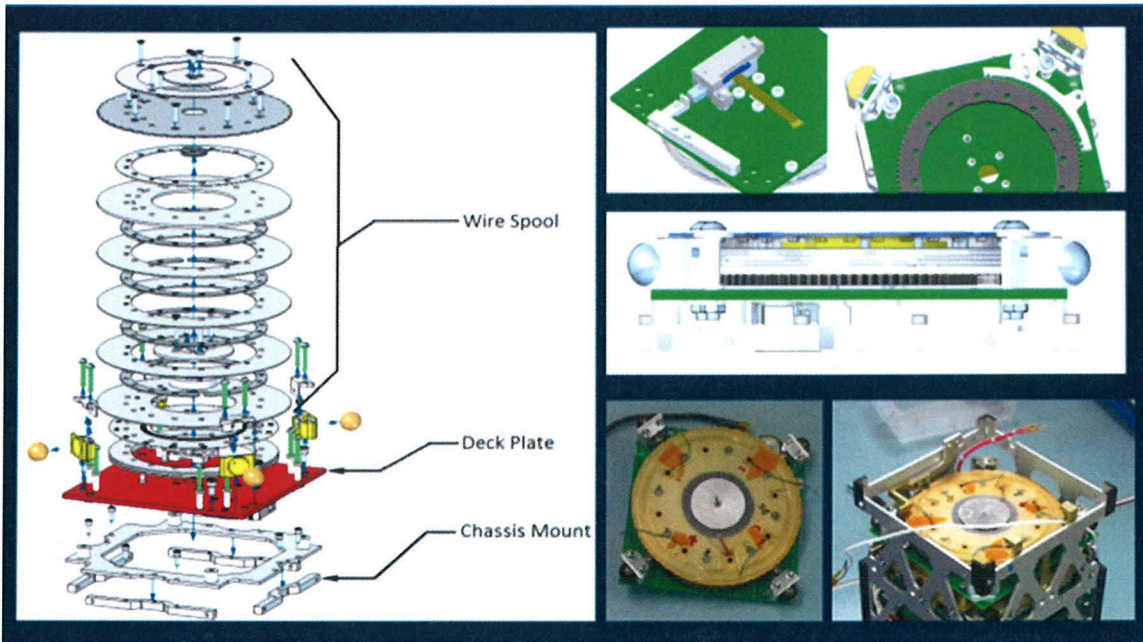

Figure 2. The DICE EFP Wire Boom Deployment Spool

Langmuir Probe (LP): The DICE LPs are used primarily to measure plasma density, N_e and N_i, and temperature, T_e. They also provide measurements of the floating potential, V_f, and space potential, V_s. The LP measurements are based on the current-voltage (I-V) response characteristics of a conductor immersed in a plasma at a Debye length or greater from surrounding structures. At Vs, the less massive electrons more easily migrate to the LP as no electric fields between the plasma and sensor surface exist. A sheath is formed around the LP sensor surface, and the resultant electric field is small and the surrounding plasma remains relatively undisturbed. Potentials applied to the LP sensor surface that are positive with respect to V_s (electron saturation region) attract and accelerate electrons. Potentials applied negative with respect to V_s (electron retarding region) begin to repel the less energetic electrons and to accelerate the ions. The V_f is the point on the I-V curve

3

when both the electron and ion flows to the LP sensor surface are equal. Potentials applied negative relative to V_f more strongly repel electrons, until a point is reached (ion saturation region) where only ions flow to the LP sensor surface, or electrons are emitted in the case of sunlit conditions. N_e and T_e can be derived from the values and slope of the electron retarding and saturation regions. N_i is determined from the value of the ion saturation region.

The Langmuir probe instrument measures electrical currents induced by charged particles striking the conductive surface of the probe. The dual Langmuir probes extend 8 cm from the spacecraft body in opposite directions along the spin axis. Once a stable spin has been established, the spacecraft also attempts to align its spin axis with the geodetic spin axis. Once spin axis alignment is achieved, the north-pointing Langmuir probe is oriented in the ram condition as the spacecraft moves toward northern latitude. This leaves the south-pointing probe following the spacecraft in its wake interfering with the measurement of charged particles. As the spacecraft passes the Earth's North Pole, the rolls of the probes is reversed and the south-pointing probe moves into the ram position.

Four brass rod booms extend 0.2 m from the four corners of the -Z face of the spacecraft. These rods comprise the UHF turnstile communications antenna. Weighted boom extensions are electrically isolated from the UHF antenna and serves only to increase the mass away from the Z-axis for spin stability.

The spacecraft deploy from the P-Pod with the Langmuir probe scissor booms and UHF antennas and extensions secured against the spacecraft body by a spring loaded lever that runs from the top to the bottom of the CubeSat. This deployment mechanism is released by a shape-memory alloy Frangibolt actuator developed by TiNi Aerospace.

The spacecraft electronics and instrumentation are tightly integrated in a stack. The electronics boards and components shown in Figure 3 are 1) the UHF communications radio and antenna interface components, 2) the electrical power system controller and battery board, 3) command and data handling (C&DH) board, 4) the Z-axis torque coil and secondary battery board, 5) attitude determination and control system (ADCS) board which includes interfaces to a sun sensor, ADCS magnetometer, GPS receiver, and Z-axis torque coil, 6) science instrument board, and 7) the electric field probe spool. The GPS antenna is located on the +Z panel. Solar panels with three solar cells each are attached on the +-X and +-Y sides of the spacecraft body. The X- and Y- torque coils are embedded in the X and Y solar panel circuit boards.

The sun sensor's aperture is exposed through small cut out in the +Z solar panel. The ADCS magnetometer is located on the ADCS electronics board within the spacecraft. The science-grade magnetometer is placed on the +Z face of the spacecraft in an attempt to distance if from the rest of the spacecraft electronics. The use of magnetic materials was kept to a minimum to avoid undesirable contamination of measurements of the Earth's magnetic field. The science magnetometer measurements are not used for in-flight attitude estimation, but comparison of the ADCs and science magnetometers on the ground serve as a confirmation of proper operation.
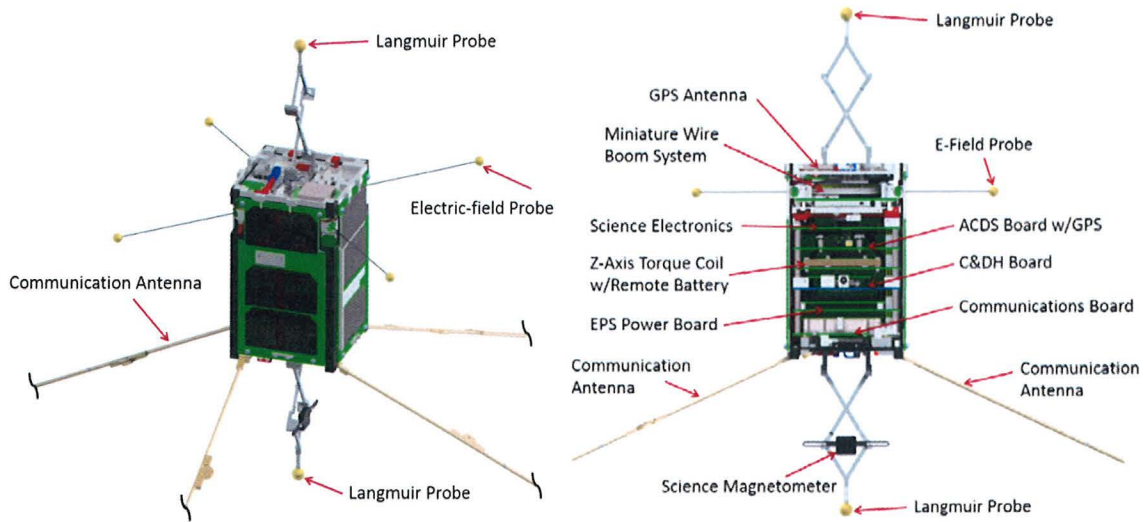
Figure 3. The DICE CubeSat Configuration

Figure 3 shows both an external and internal view of the final spacecraft solid model. Note that the E-field wire booms are shown in a partially deployed state. The cut-away view of the spacecraft shows the tightly integrated components, sensors, and electronics. The spacecraft frame serves as the principal spacecraft radiator. Temperature sensors are located throughout the CubeSat.
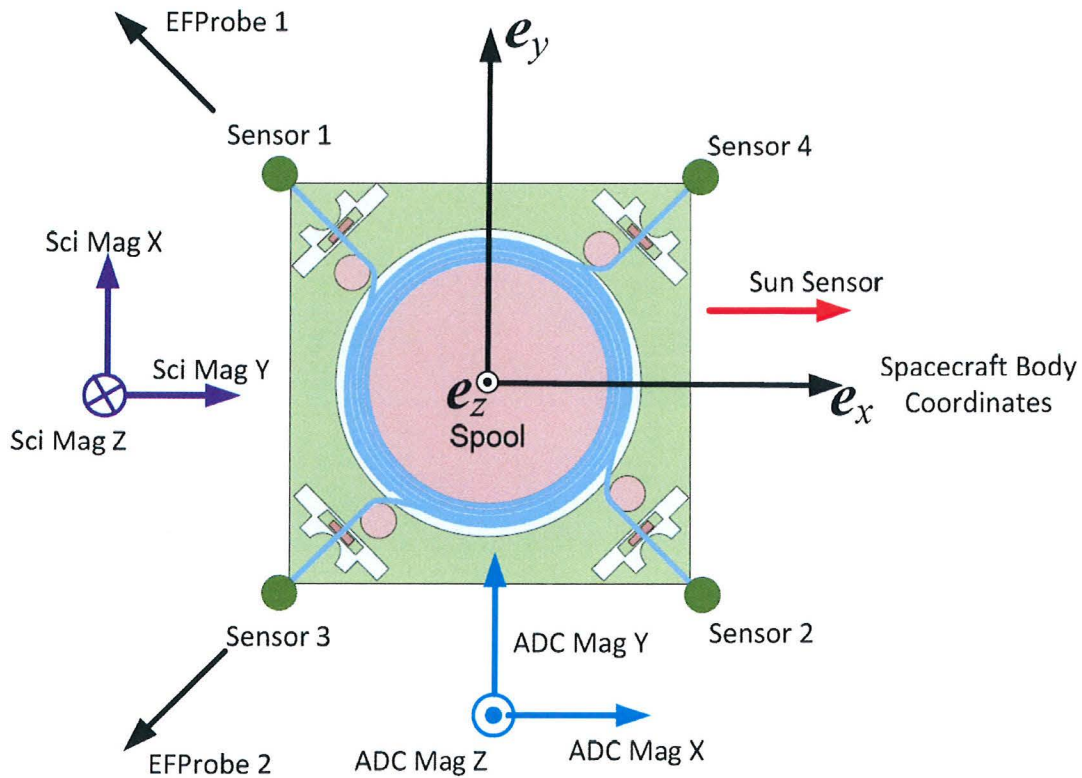

Figure 4. The DICE Spool and Sensor Map

SCIENCE RESULTS

The DICE science mission centers on the study of ionospheric space weather. Space weather refers to the ambient conditions in space and includes, but is not limited to, interactions between the Sun and the Earth's magnetosphere and ionosphere. Disturbances in space weather can affect other ground- and space-based systems including communications, surveillance and navigation systems.

DICE is focused primarily on identifying and characterizing Storm Enhanced Density (SED) features, which often occur over the United States in the afternoon. In order to better understand the formation of SED, DICE employs a suit of three electromagnetic instruments detailed above. The electric field instrument collects data to characterize the electric field found in the ionosphere. The Langmuir probe generates measurements which allow for the characterization of ionospheric plasma density. In order to properly characterize SEDs, a set of simultaneous co-located plasma density and electric field measurements must be taken as the spacecraft passes through the SED features as they develop and eventually disperse. As previously stated, the use of two identical spacecraft allows the deconvolution of the space-time ambiguity inherent to the study of space weather using in-situ measurement techniques.
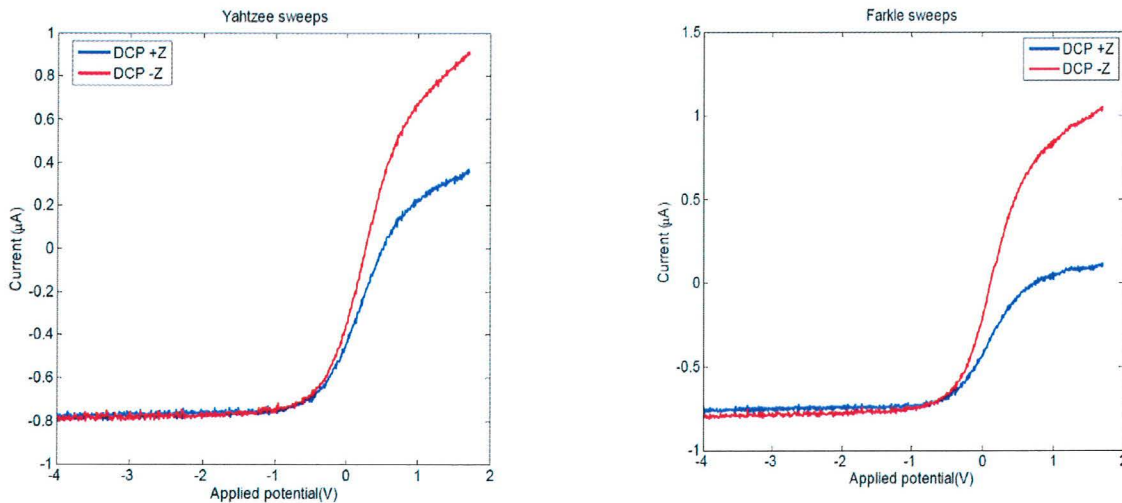
Langmuir Probe (LP) Results

Figure 5. On-orbit I-V Curves Generated by LPs

Figure 5 shows on-orbit measurements made by the Yahtzee (left panel) and Farkle (right panel) LPs. These plotted data are from the intermittent sweeps which occur every 120 s and cover a voltage range from -4 to +1.7 VDC. The shapes of these raw low noise *I-V* curves follow the projected responses and demonstrate that the LPs are operating as predicted. The difference in magnitude for the responses from the LPs on the same sensor-sat highlight that in general one of the LP sensors will be positioned more fully in the spacecraft velocity direction than the other. Thus, the higher current curves belong to the sensors that are in full or partial RAM, while the lower current curves belong to the sensors that are in a partial wake.
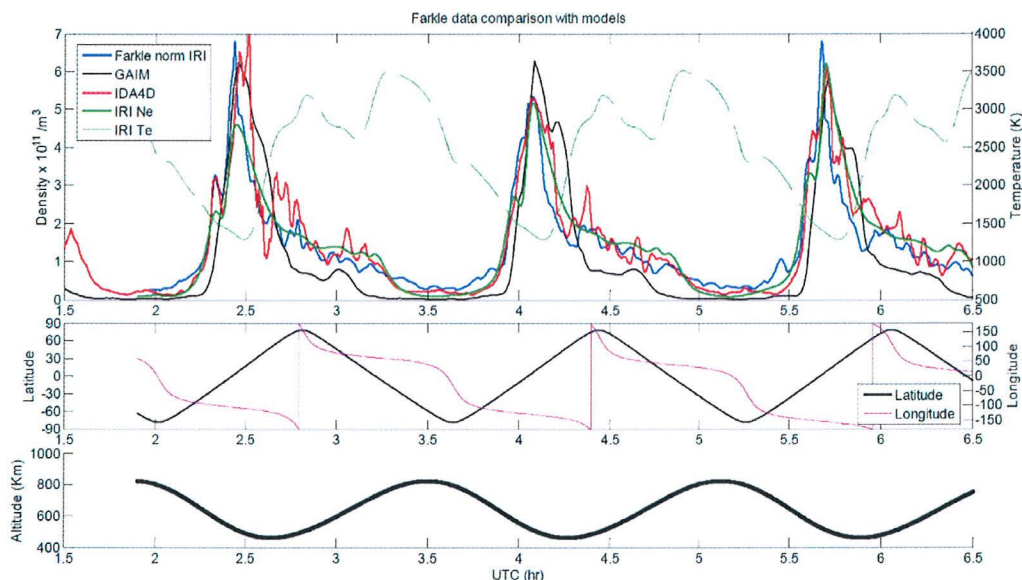
Figure 6. Comparison of Farkle LP data with the models

Figure 6 compares multi-orbit Farkle LP data from May 29th, 2012 to outputs of three ionospheric weather models; namely the Ionospheric Reference Model (IRI), ASTRA IDA4D model, and the USU Global Assimilation of Ionospheric Measurements (GAIM) model. IRI is a climatology model, while IDA4D and GAIM are nowcast assimilative models that update on a regular basis, and are forced by ingested real-time observations. USU GAIM used the Ionospheric Forecast Model (IFM) output as the initial background ionosphere, while ASTRA IDA4D used IRI 2007. Each model was run with a 15 minute time step. USU GAIM had a uniform grid of 2.5° in latitude and 15° (~ 1 hour) in longitude, whereas ASTRA IDA4D used a non-uniform grid (higher grid density over continental areas). While both models assimilated GPS TEC measurements, IDA4D also assimilated COSMIC occultation data. Due to spinning of the DICE CubeSats, and as illustrated in Figure 13, the LPs move in and out of the spacecraft wake. Therefore in order to get one density value for the data in Figure 7, we chose the maximum ion current from the two probes and then ran a smoothing filter. The fixed bias DICE LP data was normalized to the IRI data for the comparisons. The DICE LP measurements exhibit general agreement with the established ionospheric model predictions, while also demonstrating fine structure detail.
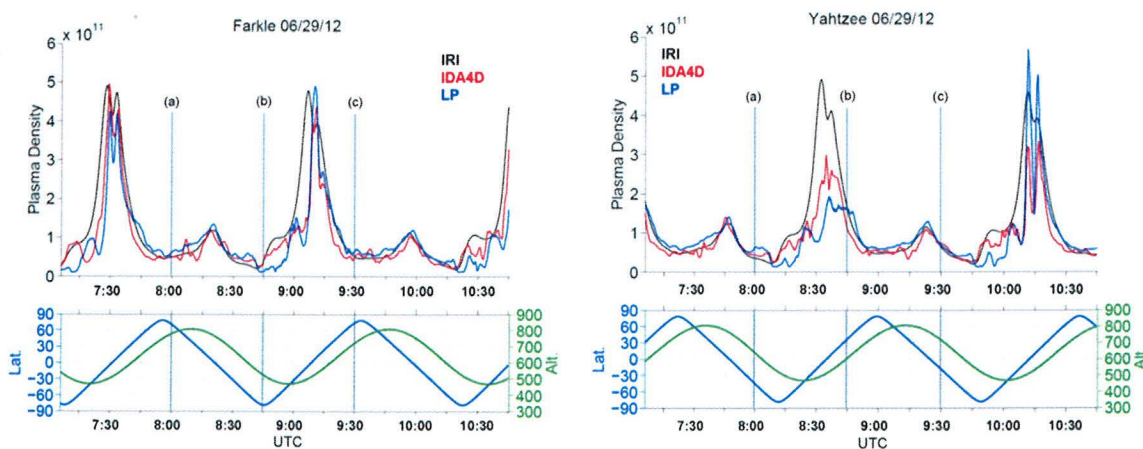

Figure 7. Simultaneous Farkle (left panel) and Yahtzee (right panel) LP Measurements
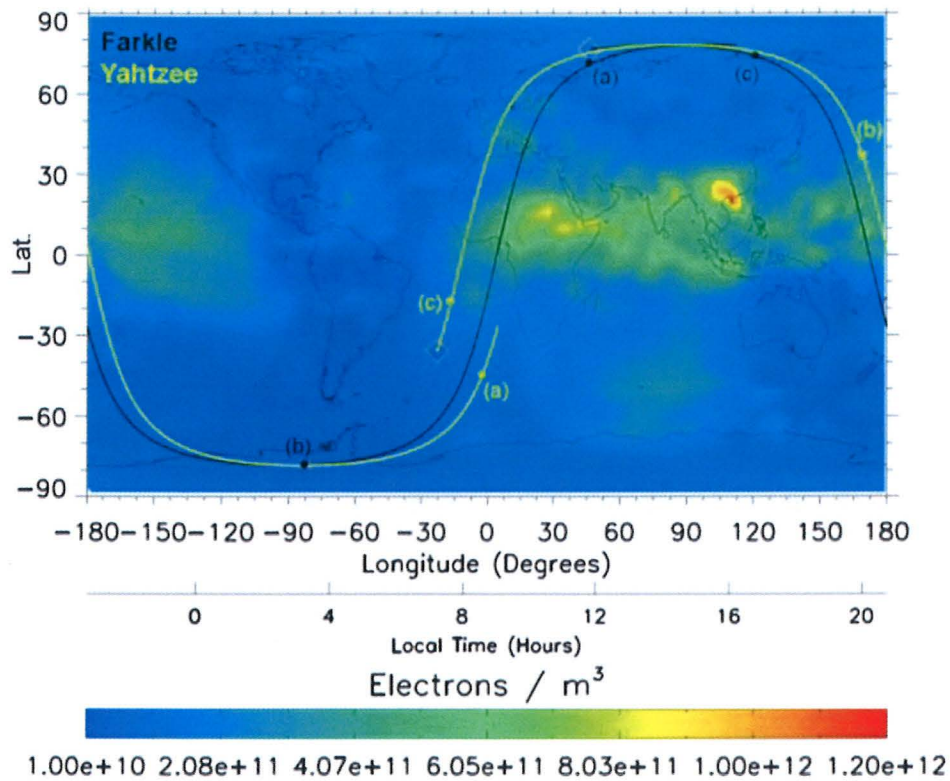
7

Figure 8. Global IDA4D Plasma Density with DICE Orbit

Figure 7 is a comparison of simultaneous measurements from both Yahtzee and Farkle and IRI and IDA4D model outputs for June 29th, 2012. The figure shows the Yahtzee and Farkle measurements against the co-located model outputs. Figure 8 provides a global reference of the DICE sensor-sat measurement tracks on top of IDA4D generated ionospheric density outputs for 500 km. The DICE orbital tracks displayed for reference; the letter annotations in the bottom panel correspond to the times marked in Figure 7. In making these figures, the two ion density DICE LP measurements for each spacecraft were averaged and then low-pass filtered and normalized to IDA4D model outputs. Once again, the DICE LP observations agrees very well with the model outputs, while not unexpectedly providing greater resolution to the overall structure. These plots also help emphasize how simultaneous measurements of spacecraft in trailing orbits can help distinguish between temporal and spatial attributes of the ionosphere. Very similar structures are seen by both spacecraft as they go through nearly identical portions of the ionosphere. However, there is also enough orbital separation (nearly half an orbit for this time of the mission), that they also fly through different portions of the ionosphere at dissimilar times and provide perspective on global spatial structure and continuity.

Science Magnetometer (SciMag) Results

The inclusion of a science-grade magnetometer (SciMag) as the third instrument allows low-noise measurements of the Earth's magnetic field, which can be correlated to the other science measurements. Comparing the science magnetometer to the ADCS magnetometer also serves to validate each of the sensors.
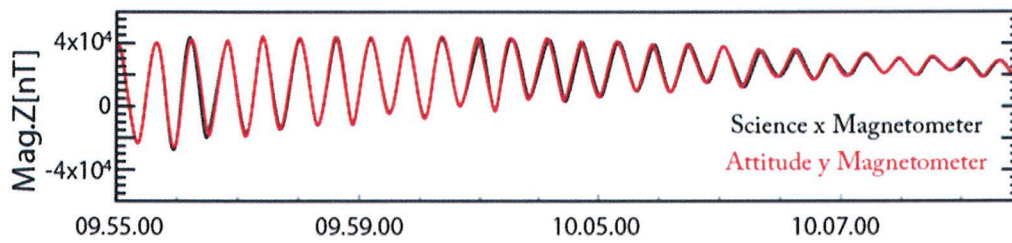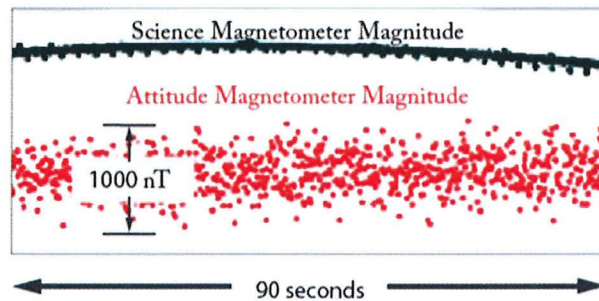
Figure 9. ADCS and Science Magnetometer Comparison

Figure 10. Close Up Magnetometer Comparison

The above figures investigate co-incident Yahtzee SciMag and ADCS magnetometer measurements acquired June 3, 2012. Figure 9 demonstrates the very good, high level agreement in the measurements from the two sensors. As they should, the signals from both sensors lay directly on top of one another. The slow tumble/spin of the spacecraft is also evident in the data. Figure 10 is a close up examination of a portion of the measurements, establishing the much lower noise floor associated with the SciMag measurements. The < 10 nT noise floor for the SciMag measurement enables detection and monitoring of geophysical disturbances and perturbations. This is clearly seen in Figure 11 which is a plot of geomagnetic activity captured by the Farkle SciMag on May 22nd, 2012. The activity is due to field aligned currents (FACs).
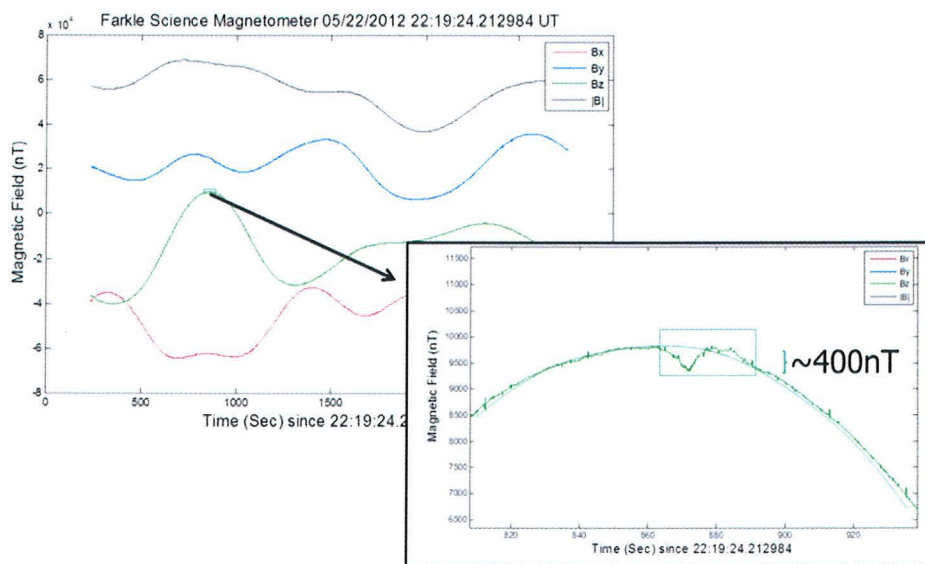

Figure 11. Geomagnetic Activity Captured by the Farkle SciMag on May 22, 2012

9

Difficulty with the deployment of the electric field probes from the wire boom spool has not allowed the intended electric field measurements to be taken. The probes of both spacecraft remain grounded in their initial, stowed location.

ADCS SUBSYSTEM OVERVIEW

ADCS on DICE is handled by the C&DH Microchip PIC24 microcontroller and the Micromega floating point unit (FPU). Due to the limited space on the FPU, simpler algorithms had to be used for the different ADCS states. Data is acquired for the ADCS algorithms via the ADCS electronics PCB. The data includes 3-axis magnetometer measurements, sun sensor vector, and GPS position and velocity measurements. The torque coil drive circuits are also located on the PCB. Because the PIC24 is inefficient at floating-point calculations, the FPU receives data and instructions from the PIC24, performs the calculations, and returns the results. These results are then used to drive the torque coils. The magnetometer and sun sensor are sampled by the data acquisition manager task every 10 Hz to feed the ADCS algorithms. The returned results are normalized and then used for pulse-width modulation firing of the torque coils.

ADCS Algorithm Design

The DICE ADCS algorithm operates in one of two states. The first state, Detumble, is entered when the spacecraft is powered on. In this state the ADCS attempts to slow spin about the X and Y axes but maintain spin about the Z axis. The spacecraft will remain in this state permanently until commanded from the ground to change states. The second state, Controller, is used when the space-craft is in a stable spin. The spin of the spacecraft can then be rotated to align with the Earth's rotational axis.

During Detumble, magnetometer measurements are used to "slow" the X and Y axes motion (in regards to the spin rate) and spin up the Z axis. Detumble uses a modified version of the B-dot algorithm. The change in the magnetic field and the required magnetic moment from the magnetic torque coils are calculated as follows:

$$\Delta \vec{B} = \vec{B} - \vec{B}_{previous} \tag{1}$$

$$\vec{M}_{detumble} = -\Delta \vec{B} \tag{2}$$

The B-dot algorithm is modified to avoid decreasing the spin rate about Z axis, as this would be an unnecessary step. This is accomplished by calculating the magnetic moment required to create a torque about the desired spin axis. The magnetic moments required to detumble and spin-up are normalized and summed along with a gain on the detumble magnetic moment.

$$\vec{M}_{command} = K_d * \left| \vec{M}_{detumble} \right| + \left| \vec{M}_{spinup} \right| \tag{3}$$

Once DICE is capable of obtaining GPS lock, the satellites could be switched to the spin stabilize mode. In this mode, the spin rate of the satellites is increased to 0.1 Hz. This is done by decreasing the gain, which allows the spin rate of the satellite to increase. DICE enters into its Con-

troller state after receiving a command from the ground. Sun sensor data, magnetometer measurements, and GPS position and velocity are used in this state. The data flow and ADCS algorithms for the Controller state is shown in Figure 12.
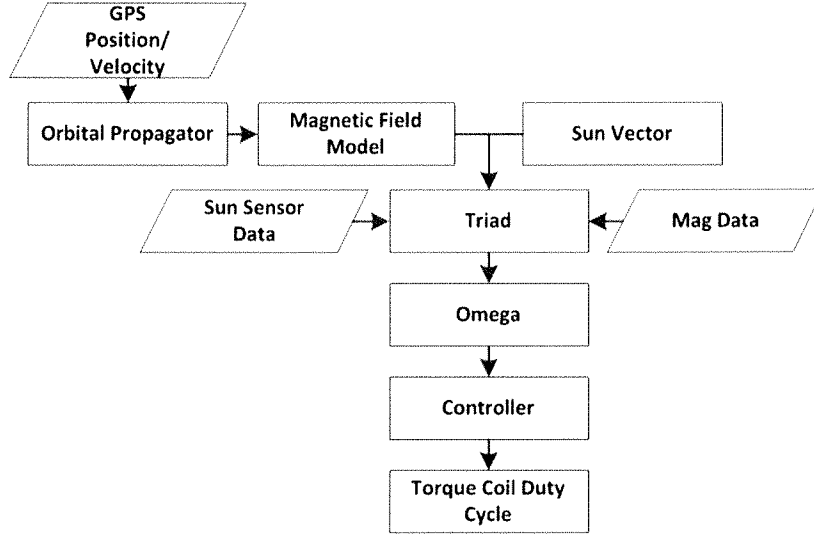

Figure 12. Data Flow and Events Diagram

Once the satellite is spin stabilized, the spin axis of the satellite is rotated to align with the Earth's nominal rotational axis. The required algorithms include triad, angular velocity estimation, sun vector, magnetic field model, onboard orbit propagator, and spin axis alignment control algorithms. The triad algorithm is used to calculate the attitude of the satellite in the form of a direction cosine matrix. The triad algorithm accepts inputs from the magnetometer ($\vec{B}^b$), the sun sensor ($\hat{s}^b$), magnetic field model ($\vec{B}^i$), and sun vector model ($\hat{s}^i$). The sun sensor data requires that the triad algorithm be run in sunlight. Six basis unit vectors are created using the following equations where (x) is (b) or (i), depending on whether the data originates from the sensors or the model.

$$\hat{\imath}_1^x = \hat{s}^x \tag{4}$$

$$\hat{\imath}_2^x = \frac{\hat{s}^x \times \vec{B}^x}{\left|\hat{s}^x \times \vec{B}^x\right|} \tag{5}$$

$$\tag{6}$$

$$\hat{\imath}_3^x = \hat{\imath}_1^x \times \hat{\imath}_2^x$$

These basis vectors create two direction cosine matrices and the attitude of the spacecraft:

$$R_i^b = [\hat{\imath}_1^b \quad \hat{\imath}_2^b \quad \hat{\imath}_3^b][\hat{\imath}_1^i \quad \hat{\imath}_2^i \quad \hat{\imath}_3^i]^{-1} \tag{7}$$

The current and previous direction cosine matrices are used to calculate the angular velocity. A direction cosine matrix that describes the rotation of the satellite from its previous attitude to its current attitude can be calculated as follows:

11

$$R_{previous \rightarrow current} = \left[R_i^b \right]_{current} * \left[R_i^b \right]_{previous}^{-1} \qquad (8)$$

The direction cosine matrix is simplified if the rotation between the two times is assumed to be small.

$$R_{previous \rightarrow current} \approx \begin{bmatrix} 1 & \Delta\theta_z & -\Delta\theta_y \\ -\Delta\theta_z & 1 & \Delta\theta_x \\ \Delta\theta_y & -\Delta\theta_x & 1 \end{bmatrix} \qquad (9)$$

This simplification reduces the rotation matrix to small angular changes about the spacecraft's X, Y, and Z axes. The angular velocity of the satellite is calculated by approximating the time derivative of these small angles.

$$\vec{\omega}_{b/i}^b \approx \begin{bmatrix} \dfrac{\Delta\theta_x}{\Delta t} \\ \dfrac{\Delta\theta_y}{\Delta t} \\ \dfrac{\Delta\theta_z}{\Delta t} \end{bmatrix} \qquad (10)$$

A simple sun vector algorithm calculates the expected location of the Sun in the J2000 inertial coordinate system (Vallado 2001). It accepts the current Modified Julian Date as an input, and outputs the expected unit vector to the sun. The Modified Julian Date is calculated from GPS time, when GPS is available, or from the onboard clock. The expected local magnetic field vector is calculated using a simple dipole model derived from the 2010 World Magnetic Model (WMM). The WMM requires the satellites current position as an input. When GPS position is unavailable, it is calculated using a simple onboard two-body orbit propagator.

$$\dot{\vec{r}}^i = \dot{\vec{v}}^i$$

$$\qquad (12)$$

$$\dot{\vec{v}}^i = -\frac{\mu_{earth}}{|\vec{r}^i|^3} * \vec{r}^i$$

$$\qquad (11)$$

The spin axis of the satellite is aligned by controlling the angular momentum vector of the satellite. The angular momentum of the satellite in a satellite body coordinate system is approximated by assuming the body coordinate system is aligned with the principal axes of inertia:

$$\vec{h}^b \approx \begin{bmatrix} I_{xx}^b * \omega_x^b \\ I_{yy}^b * \omega_y^b \\ I_{zz}^b * \omega_z^b \end{bmatrix} \qquad (13)$$

The angular momentum of the satellite is rotated to the inertial J2000 coordinate system by multiplying the direction cosine matrix, calculated using the triad algorithm, with the angular momentum in the satellite body coordinate system:

$$\vec{h}^i = R_b^i * \vec{h}^b \qquad (14)$$

The torque required to align the spin axis and maintain the current spin rate is calculated in the inertial coordinate system. This is then rotated back to the satellite body coordinate system:

$$\vec{T}^i_{align} = -K_h * \begin{bmatrix} h^i_x \\ h^i_y \\ h^i_z - I^b_{zz} * \omega_{desired} \end{bmatrix} \tag{15}$$

$$\vec{T}^b_{align} = R^b_i * \vec{T}^i_{align} \tag{16}$$

The torque to dampen the satellite's nutation is calculated in the body coordinate system of the satellite:

$$\vec{T}^b_{nutation} = \begin{bmatrix} -K_x * \omega^b_x \\ -K_x * \omega^b_y \\ -K_z * (\omega^b_z - \omega_{desired}) \end{bmatrix} \tag{17}$$

The two calculated torques are summed together providing the magnetic moment required to generate the torque:

$$\vec{T}_{command} = \vec{T}^b_{align} + \vec{T}^b_{nutation} \tag{18}$$

$$\vec{M}_{command} = \frac{\vec{B} \times \vec{T}_{command}}{|\vec{B}|^2} \tag{19}$$

After the spin axis has been aligned, the spin rate of the satellite is increased, up to 2 Hz, to allow boom deployment. This is accomplished by increasing the desired spin rate ($\omega_{desired}$) in the spin axis alignment algorithm. The spin rate decreases as the booms are deployed. To compensate, the satellite spin rate increases to continue deployment. Figure 13 shows DICE in its final spinning state.

MAJOR-AXIS SPINNING

The DICE team faced several design and operational challenges associated with the requirement for a spinning spacecraft. Great consideration was given to designing a spacecraft that tends to spin naturally about the desired axis. GPS constellation simulation testing was also performed to ensure the spin of the spacecraft would not excessively degrade the GPS signal acquired by the GSP receiver. These two design and test efforts are detailed below.
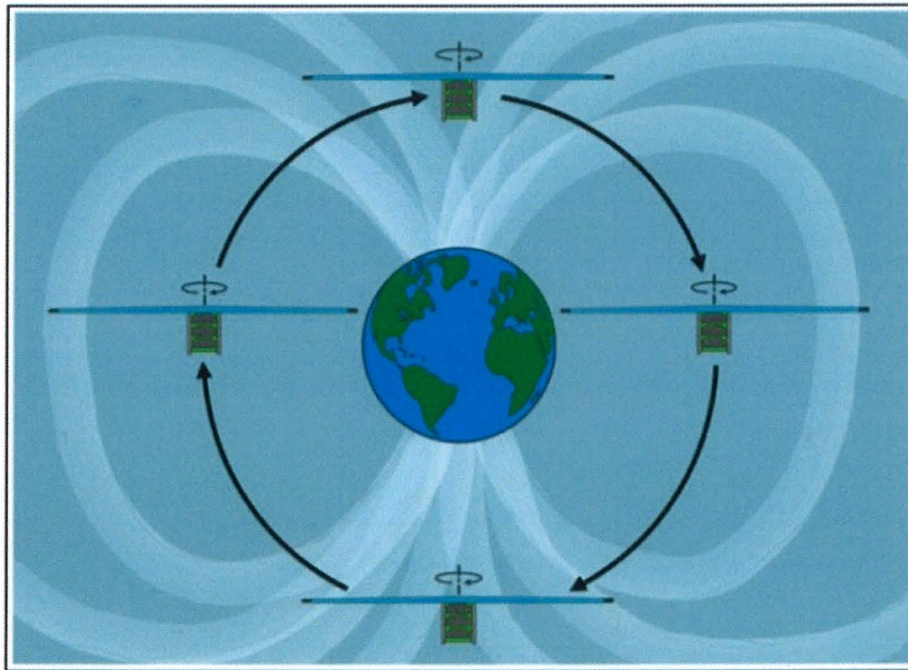
Figure 13. Axis Alignment & Spin

Challenges of spinning a 1.5 U CubeSat

One of the major design challenges faced by the DICE team was the need to achieve spin stability about the longest spacecraft axis. The desired spin axis was defined by the plane of the EFP spool. For a simple 10 x 10 x 15 cm body, the natural direction of spin would tend to have the spacecraft toppling end-over end.

A rigid body spinning in free space is considered a "major-axis spinner" when spinning about the largest of its principal moments of inertia (MOI). Major-axis spin is the lowest energy state possible and results in stable rotational motion. In this state, the body's spin rate decreases steadily due to energy loss mechanisms—the largest of which is magnetic eddy currents interacting with the Earth's magnetic field. The response of a rigid body to an external torque applied perpendicular to the angular momentum is a shift of the instantaneous rotation vector resulting in the well-known coning or precession of the body axis in space about the angular momentum vector. This type of motion implies that the spacecraft has additional energy above the lowest energy state. Over time this energy will be dissipated, principally through slight flexures of the various booms as well as damping washers the wires pass through as the wires leave the corners until the spacecraft returns to the minimum energy state, with simple spinning motion about the major axis of inertia.

For DICE, extending the Langmuir probe scissor booms along its already longer axis only worsens the problem. In order to increase the X and Y moments of inertia, additional mass was required away from the Z-axis. This mass was added using extensions to the UHF communications antenna. When deployed, these antennas increase the moments of inertia somewhat about the desired spin axis. However, in order to further increase the moments of inertia and ensure the spacecraft's spin stability about the desired spin axis, additional hinged brass segments with tungsten inserts were added to the UHF segments as weighted extensions. These boom extensions are electrically isolated from the UHF antenna and serves only to increase the mass away from the Z-axis.

14

GPS Constellation Simulations

Each DICE spacecraft is equipped with a NovAtel OEMV-1 GPS receiver as well as a WySys GPS L1 patch antenna. The GPS receiver provides position and velocity data to the ADCS system as well as precise time to the entire spacecraft. Due to the ~1 W power consumption of the GPS receiver and antenna LNA, the GPS must be duty-cycled to conserve power—nominally every 3 hours. The GPS is said to "cold start" if it has been powered down for more than 2 hours, meaning that any previously downloaded ephemeris is deemed too stale for use and a the current ephemeris must be acquired. Lab testing of the receiver with a rooftop antenna showed an average cold start time (from power on, to position/velocity solution) of less than 100 s. However, acquiring a GPS signal lock from an orbiting, spinning platform presents additional challenges that are not easy to test in a lab without the use of a GPS constellation simulator.

From an orbiting platform, high signal Doppler impedes the ability of the receiver to converge on a solution. However, a typical LEO orbit provides a better view of the GPS constellation with little-to-no atmospheric effect. Furthermore, since patch antennas are inherently not omnidirectional, the placement of a GPS patch antenna on a spinning spacecraft is critical. As a spacecraft spins about a single axis or tumbles about all axes, a patch antenna which cannot maintain the same set of GPS spacecraft in view for more than a few seconds is unlikely to achieve a valid position/velocity solution.

For DICE, placing the GPS patch antenna on either of the ±Z panels gives the antenna a "view" of the constellation that rotates but maintains the same GPS spacecraft in view for several minutes allowing the receiver to acquire the GPS constellation ephemeris and arrive at a precise position/velocity solution.
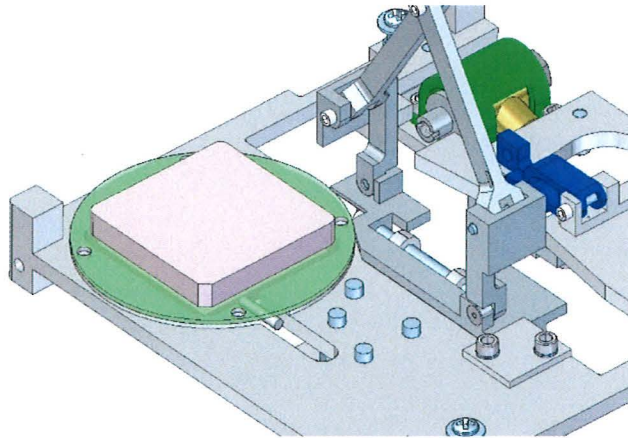

Figure 14. GPS L1 Patch Antenna Shown in DICE Solid Model

Figure 14 shows the GPS patch antenna (near left corner with circular, green ground plane) mounted on the +Z spacecraft face. The LP scissor boom, partially shown extending up away from the plate, is made of Delrin and does not interfere substantially with the antenna pattern.

In order to test and validate the ability of the GPS receiver to acquire the ephemeris and position/velocity solutions as observed from a spinning spacecraft such as DICE, GPS constellation simulation testing was performed. Use of the NASA Goddard Space Flight Center (GSFC) GPS simulator allowed the DICE team to test the performance of the GPS receiver (Figure 15). Multiple simulation scenarios were created to vary the orbital altitude (350 vs. 800 km), spin rate (1 Hz vs. 0.1 Hz), and spin type (controlled vs. tumble) the GPS receiver would perceive.
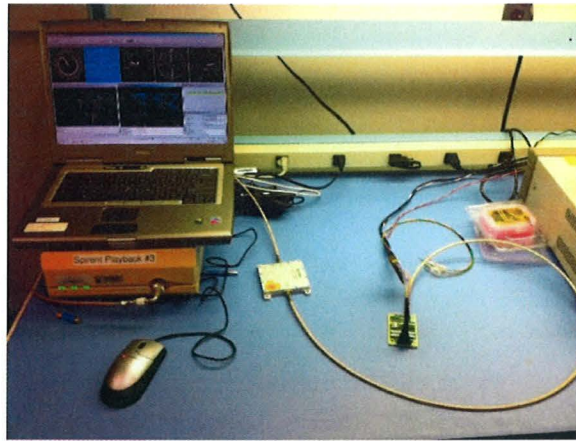
Figure 15. GSFC Test Setup

In GPS simulation testing, all scenarios involving a tumbling spacecraft struggled to achieve a signal lock. However, consistent position/velocity solutions could be achieved in all other scenarios regardless of the other test parameters (altitude and spin rate). The cold-start time-to-lock ranged from 75 to 810 seconds with an average of 401 seconds. By comparison, ground testing of the same unit, when not in motion, showed an average cold start of less than 100 seconds.
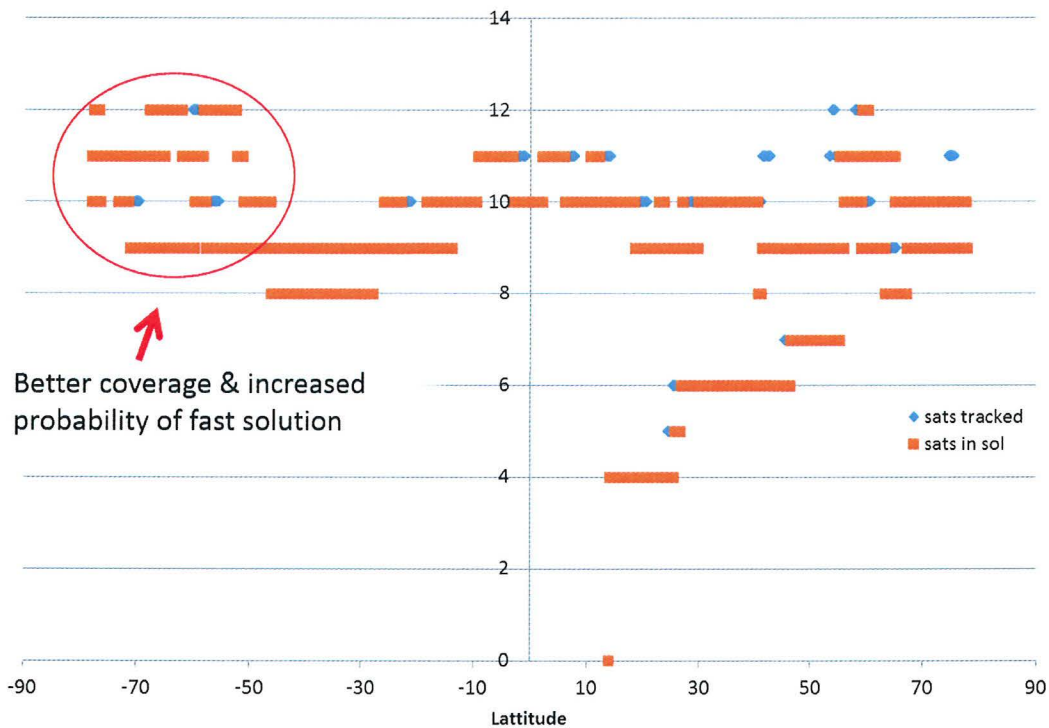

Figure 16. GPS Satellites Tracked Correlated to Latitude

An interesting result from GPS simulation testing was found for all simulation scenarios involving proper spin and geodetic axis alignment. The number of GPS spacecraft in view on average correlates to the of spacecraft latitude when the receiver begins its cold start and solution acquisition time. The data collected for this scenario showed better constellation coverage and shorter cold

16

start times. Better solution acquisition times were achieved on average when cold start was initiated at lower latitudes around the Earth's South Pole. Keeping in mind that the GPS patch antenna is on the +Z face of the spacecraft, and that under nominal, geodetically aligned spin that points the antenna principally in the nadir direction, the improved lock times might seem counter-intuitive. In other words, when the antenna is pointed in the nadir direction more of the GPS constellation tends to be in view around the edges of the Earth than in an "unobstructed," anti-nadir orientation (Figure 16).

ADCS CHALLENGES

While on-orbit operations of both spacecraft were successful across most of the mission objectives, a few specific operational challenges precluded the deployment of the EFP wire booms on either of the two spacecraft. These operational difficulties are detailed below.

Farkle's Center of Mass / MOI Off

Great care was given during the design, assembly and test phases of the program to estimate and control and measure each spacecraft's center of mass (CoM) and moments of inertia. Once the spacecraft were deployed, the ADCS algorithm was engaged and the spacecraft began returning ADCS algorithm metrics and pointing data, it became apparent that one of the DICE spacecraft (Farkle) was not responding as anticipated. From data gathered from Farkle's telemetry, new estimates of the on-orbit moments of inertia have been generated—unfortunately, the do not match the ground measurements. It is thought that, perhaps, the weighted boom segments did not all deploy properly shifting the center of mass and decreasing the X and Z moments of inertia.

Considerable time and effort have been spent attempting to correct Farkle's spin. The ADCS system is able to coerce Farkle closer to a proper spin. However, the inherent spin instability of the spacecraft eventually causes the improved spin to degenerate and the spacecraft returns somewhat of a tumbled spin. Without a proper spin about the Z axis, the Farkle spool is unable to deploy. This issue has not reduced the functionality of any of the other Farkle instruments or subsystems and Farkle continued to function and to date has returned 5.13 gigabytes of valuable science, ADCS, and housekeeping data to the ground.

The second spacecraft, Yahtzee, had on-orbit MOI estimates much closer to values measured on the ground. With Yahtzee, the DICE team has been able to achieve a much more stable spin about the Z-axis.

Critical Sequence of Events for Geodetic Axis Alignment.

In order for the CubeSat to align with the geodetic axis as desired, a critical sequence of ADCS events most occur. When the spacecraft are first ejected from the deployment pod, they are in an uncontrolled, tumbling state. One of the primary reasons for the two distinct ADCS modes mentioned above, is that the Controller algorithm requires orbital position/velocity data which, is provided by the GPS receiver. However, the GPS receiver has little chance of acquiring the needed information without the spacecraft entering a stable spin first. In other words, in order for DICE to achieve its eventual goal of geodetic axial alignment, the spacecraft must attain a controlled spin about the +Z axis first, then acquire its position/velocity, and finally be commanded from the ground to enter the Controller state where the spin is maintained, but gradually shifted into the proper alignment.

Lapses in Communication

The final operational challenge which made deployment of the EFP wire booms difficult, for Yahtzee in particular, was an issue with making consistent contact with the operations center. After

the first several months of operations, which were used for spacecraft checkout procedures, Yahtzee stopped responding for several days but then returned to nominal operations. It became apparent that during the communications lapse, the spacecraft had reset and the torque coils had been disabled causing the previously achieved spacecraft spin rate to decay.

The communication lapse was attributed to anomaly of the spacecraft electronics due to the space environment. Unfortunately, the lapses in communication became common to both spacecraft—although more frequent with Yahtzee. These lapses contributed much of the difficulty with the spin-up of Yahtzee. Several times during mission ops, the proper spin rate was achieved deployment of the EFP spool was impeded by another anomaly.

Despite the lapses in communication, Yahtzee continued to function and to date has returned 3.26 gigabytes of valuable science, ADCS, and housekeeping data to the ground.

ADCS SUCCESSES

Overall, the DICE ADCS system performed very well and provided valuable advances to the SDL team for future missions. Some points of success are summarized below.

Pointing Control

As with many CubeSats, the DICE attitude determination and control system is relatively simple and the power budget quite constrained. With only torque coils and limited power to actuate them, extensive simulations and ground testing were performed to ensure that the spacecraft would have sufficient torque authority to control spacecraft spin and alignment. The power delivered to the torque coils (and by extension, the torque authority of the spacecraft) were made configurable to allow mission operators to balance power considerations with torque authority.

Throughout the DICE mission the torque authority was shown to be very healthy. For much of the on-orbit operations, power/torque authority were scaled to 10-15% of full scale. This was shown to be adequate for detumble and spin maintenance maneuvers which were allowed to last for one to three days. When faster reaction times were desired, the scale factor was increased to 20% - 30% decreasing the reaction times of ADCS commands, but with essentially similar end results.

Pointing Knowledge

The DICE spacecraft use measurements from an ADCS magnetometer and an SDL designed sun sensor to estimate and control the orientation and spin of the spacecraft. The sun sensor is key to controlling the spin rate and spacecraft spin axis orientation. Sun sensor data is also critical to performing highly accurate science data analysis. The DICE sun sensors have performed very well on orbit, exceeding expectations. Figure 17 shows the Yahtzee ADCS sun sensor measurement performance as determined from the first few months of operation. The sun sensor is providing on-orbit accuracies of around 0.15°—far better than the predicted levels of ~ 0.7°.
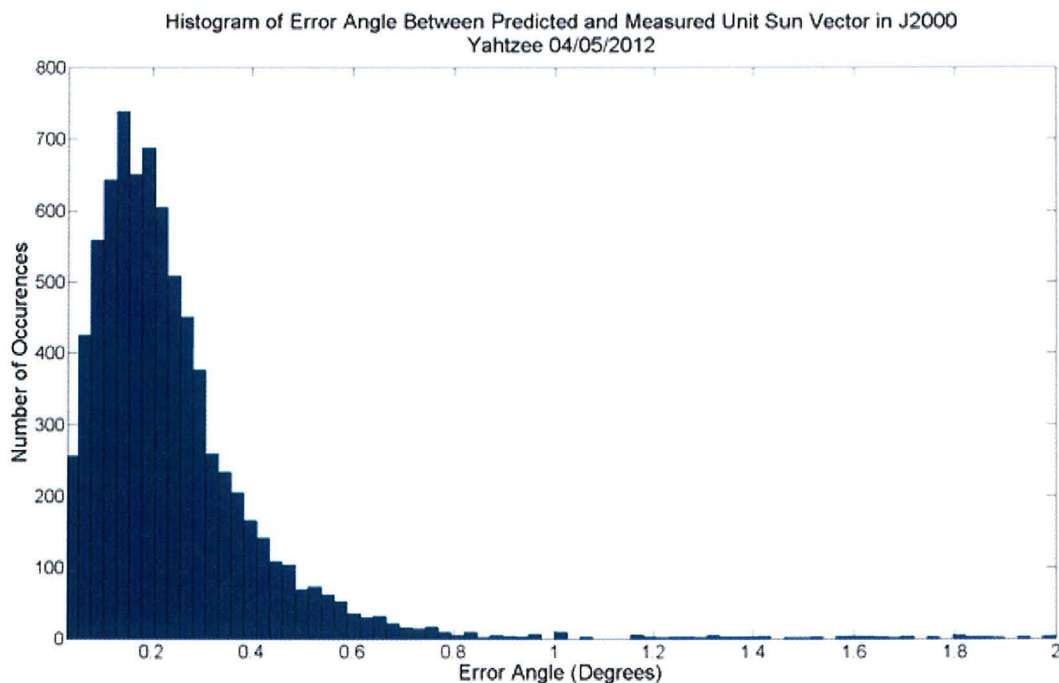
Figure 17. DICE Sun Sensor Pointing Error

Yahtzee's Performance as a Spinning Spacecraft

The repeated successful spin-up of Yahtzee demonstrates the ability of a relatively simple ADCS system, with only torque coils for attitude control, to achieve spin stability of a 1.5U CubeSat up to 2 Hz.

CONCLUSIONS

The DICE mission has demonstrated a number of first ever science measurements from a CubeSat, including multi-platform measurements of Langmuir Probe and Science Magnetometer measurements. These successful demonstrations of science grade measurements from a CubeSat are notable first step in a pathfinder process to low-cost, multi-point CubeSat constellation observations of the Sun-to-Earth system. DICE has also enabled a number of groundbreaking technologies to the CubeSat community. Most notably has been the development and demonstration of a multi-Mb/s downlink radio for use on regularly licensed bands. This development includes not only the design and implementation of the high-speed space to ground CadetU radio, but also the tools, facilities, and infrastructure to provide the ground tracking, communication link closure, and data acquisition and management on the ground. This has come in large part to the teaming with L-3 Communications and NASA WFF. DICE has also promoted and demonstrated a miniature, reliable CubeSat deployment mechanism actuator based on the TiNi SMA technology.

The DICE ADCS in particular demonstrated the ability of CubeSat missions to achieve and maintain spin stability and precise alignment with relatively simple hardware and software and with a constrained power budget. Future missions will be able to leverage substantial ADCS mechanical and electrical design work, algorithm development, hardware-in-the-loop test facilities, and on-orbit operational experience gained by the program. Advances in miniaturized magnetometers, sun sensors, torque coils, processing hardware, and algorithms have advanced the state-of-the-art for

19

miniaturization of spacecraft systems as the industry advances toward smaller spacecraft and smaller ADCS solutions.

The success of the DICE mission has spurred the development of two on-going DICE-related programs in preparation for the larger multi-point CubeSat constellation observations of the Sun-to-Earth system. The first is the AFRL sponsored Double-probe Instrument for Measuring E-fields (DIME) SBIR program. ASTRA LLC and USU/SDL have teamed on this program to further enhance the design for the measurement of electric fields from CubeSat sized spacecraft. The DIME program leverages the DICE design and lessons learned to improve upon the EFP boom deployment and spacecraft stability designs. Notably, the DIME EFP boom deployment mechanism employs a piezo-electric motor for simple, controlled release and retraction of the EFP booms. It utilizes the general spool approach developed on DICE, but employs a number of stabilizing and locking mechanisms that improve upon the design and also locates the spool in the middle of the spacecraft stackup. These enhancements will greatly aid in test and calibration of the sensor before flight. Additionally, the spacecraft design has been modified to strongly emphasize a more dominant spin axis about the sensor-sat Z axis, which will be aligned with the geodetic axis. The DIME spacecraft is expected to launch in 2016, following a successful completion of the SBIR.

The second is the NASA sponsored Auroral Spatial Structures Probe (ASSP) sounding rocket program, which is a mission to measure both the spatial and temporal variation of the energy flow into the upper atmosphere in and around the aurora. ASSP is led and implemented by USU/SDL, with science support from ASTRA. The data from ASSP will be combined with ground-based observations of winds, large-scale electric field patterns, and auroral images. ASSP will be launched in 2015 from Poker Flats, AK during geo-magnetically active conditions and just before the onset of an auroral sub-storm. To capture the data, ASSP will use a constellation of six small sub-payloads, ejected in a spinning state from a main payload, which are similar in design and functionality to the DICE spacecraft. Each of the six sub-payloads and the main payload carry a crossed pair of EFP sensors to measure *in-situ* electric fields, a three axis SciMag, a LP, and a GPS receiver. The data obtained at the different spatial locations and baselines will be used to develop models for the spatial and temporal distribution of electric fields and their correlations in space and time.

ACKNOWLEDGMENTS

REFERENCES

[1] Chad Fish et al, "Design, Development, Implementation, and On-orbit Performance of the Dynamic Ionosphere CubeSat Experiment Mission" (SPAC-D-13-00035R2) *Space Science Review*.